Sasaki H, Yabe I, Tashiro K (2003) The hereditary spinocerebellar ataxias in Japan. Cytogenet Genome Res 100:198–205

Schols L, Bauer P, Schmidt T, Schulte T, Riess O (2004) Autosomal dominant cerebellar ataxias: clinical features, genetics, and pathogenesis. Lancet Neurol 3:291–304

Shimizu Y, Yoshida K, Okano T, Ohara S, Hashimoto T, Fukushima Y, Ikeda S (2004) Regional features of autosomal-dominant cerebellar ataxia in Nagano: clinical and molecular genetic analysis of 86 families. J Hum Genet 49:610–616

Takashima M, Ishikawa K, Nagaoka U, Shoji S, Mizusawa H (2001) A linkage disequilibrium at the candidate gene locus for 16q-linked autosomal dominant cerebellar ataxia type III in Japan. J Hum Genet 46:167–171

Van Swieten JC, Brusse E, de Graaf BM, Krieger E, van de Graaf R, de Koning I, Maat-Kievit A, Leegwater P, Dooijes D, Oostra BA, Heutink P (2003) A mutation in the fibroblast growth factor 14 gene is associated with autosomal dominant cerebellar ataxia [corrected]. Am J Hum Genet 72:191–199

Zhuchenko O, Bailey J, Bonnen P, Ashizawa T, Stockton DW, Amos C, Dobyns WB, Subramony SH, Zoghbi HY, Lee CC (1997) Autosomal dominant cerebellar ataxia (SCA6) associated with small polyglutamine expansions in the alpha 1A-voltage-dependent calcium channel. Nat Genet 15:62–69

Cell Death and Differentiation (2007) 14, 2058–2067

www.nature.com/cdd

Bax-inhibiting peptide protects cells from polyglutamine toxicity caused by Ku70 acetylation

Y Li[1,5], T Yokota*[,1,5], V Gama[2], T Yoshida[1,2], JA Gomez[2], K Ishikawa[1], H Sasaguri[1], HY Cohen[3], DA Sinclair[4], H Mizusawa[1] and S Matsuyama*[,2]

Polyglutamine (polyQ) diseases, such as Huntington's disease and Machado–Joseph disease (MJD), are caused by gain of toxic function of abnormally expanded polyQ tracts. Here, we show that expanded polyQ of ataxin-3 (Q79C), a gene that causes MJD, stimulates Ku70 acetylation, which in turn dissociates the proapoptotic protein Bax from Ku70, thereby promoting Bax activation and subsequent cell death. The Q79C-induced cell death was significantly blocked by Ku70 or Bax-inhibiting peptides (BIPs) designed from Ku70. Furthermore, expression of SIRT1 deacetylase and the addition of a SIRT1 agonist, resveratrol, reduced Q79C toxicity. In contrast, mimicking acetylation of Ku70 abolished the ability of Ku70 to suppress Q79C toxicity. These results indicate that Bax and Ku70 acetylation play important roles in Q79C-induced cell death, and that BIP may be useful in the development of therapeutics for polyQ diseases.
Cell Death and Differentiation (2007) **14**, 2058–2067; doi:10.1038/sj.cdd.4402219; published online 21 September 2007

Nine inherited neurodegenerative disorders with expanded polyglutamine (polyQ) are caused by mutations in different genes, but they likely share the common pathology in which expanded polyQ gains toxic functions.[1] The molecular mechanism of neuronal toxicity of polyQ remains enigmatic. Recent findings suggest that the intracellular aggregation of polyQ causes cellular stress responses that trigger neuronal cell death.[1] It is hypothesized that polyQ aggregation suppresses neuronal transcriptional activity by sequestering histone acetyltransferases (HAT) from chromosomes and thus polyQ causes neuronal cell death.[2–4]

Bax is a proapoptotic member of Bcl-2 family proteins that plays a key role in programmed cell death in neurons.[5,6] Recently, mutant huntingtin with expanded polyQ was shown to activate p53 and increase the expression level of Bax.[7] Based on these previous findings, we became interested in examining the role of Bax in polyQ-induced cell death. Recently, we developed a series of cytoprotective membrane-permeable pentapeptides that rescue cells from Bax-mediated cell death. These peptides are named Bax-inhibiting peptides (BIPs) and were designed from the Bax binding domain of Ku70.[8–10] Ku70 is a multifunctional protein playing roles in DNA repair and cell survival.[11] Ku70 has been shown to inhibit Bax-mediated cell death by binding Bax in the cytosol.[12–14] The present study demonstrates that BIP can rescue cells from polyQ toxicity, and that polyQ promotes Bax-mediated cell death by inducing Ku70 acetylation that activates Bax.

Results

BIP suppresses Q79C-induced cell death. BIPs consisting of five amino acids (e.g. VPMLK and VPTLK) were used in this study. A mutated peptide (i.e. IPMIK) that does not bind Bax but retains cell permeability was also used in this study as a negative control (NC). For the investigation of polyQ toxicity, we used the C-terminal, truncated fragment of the Machado–Joseph disease 1 (MJD1) gene product, ataxin-3, which includes an expanded polyQ stretch (79 glutamine repeats, Q79C).[15,16] As a negative control, ataxin-3 C-terminus with 22 or 35 glutamine repeats (Q22C and Q35C, respectively) was used.[15,16] BIP readily suppressed Q79C-induced cell death in a neuroblastoma cell line (Neuro-2a) (Figure 1a and b) and in a human embryonic kidney cell line (HEK293T) (Figure 2a). Although these cell lines incorporated BIP very efficiently,[9] the primary cultured rat cortical neurons showed very low uptake of BIP. To study whether BIP can suppress polyQ-induced cell death in primary cortical neurons, we utilized the protein transduction domain of the human immunodeficiency virus (HIV) trans-activator (TAT)[17] to enhance cell permeability of BIP. PolyQ was expressed by an adenovirus vector.[16] We confirmed that TAT-BIP efficiently entered primary cortical neurons (Supplementary Figure 1), and it inhibited polyQ-induced cell death in these cells (Figure 1c). To confirm the role of Bax in polyQ-induced cell death, we employed small interference RNA (siRNA) targeting Bax mRNA (Figure 1d).

[1]Department of Neurology and Neurological Science, Tokyo Medical and Dental University, Tokyo, Japan; [2]Departments of Medicine and Pharmacology, Case Western Reserve University, Cleveland, OH, USA; [3]Faculty of Life Sciences, Bar-Ilan University, Ramat-Gan, Israel and [4]Paul F. Glenn Laboratories for the Molecular Biology of Aging, Department of Pathology, Harvard Medical School, Boston, MA, USA
*Corresponding authors: T Yokota, Department of Neurology and Neurological Science, Tokyo Medical and Dental University, Tokyo 113-8519, Japan. Tel: +81 3 5803 5234; Fax: +81 3 5803 0169; E-mail: tak-yokota.nuro@tmd.ac.jp or S Matsuyama, Departments of Medicine and Pharmacology, Case Western Reserve University, Cleveland, OH 44106, USA. Tel: 216 368 5832; Fax: 216 368 8919; E-mail: shigemi.matsuyama@case.edu
[5]These authors contributed equally to this work
Keywords: polyglutamine; Bax; Ku70; Acetylation; SIRT1
Abbreviations: polyQ, polyglutamine; MJD, Machado–Joseph disease; BIP, Bax-inhibiting peptide; LDH, lactate dehydrogenase; siRNA, small interference RNA; CBP, cyclic-AMP response element-binding protein; HDAC, histone deacetylase; TSA, trichostatin A
Received 22.12.06; revised 23.7.07; accepted 23.7.07; Edited by M Deshmukh; published online 21.9.07

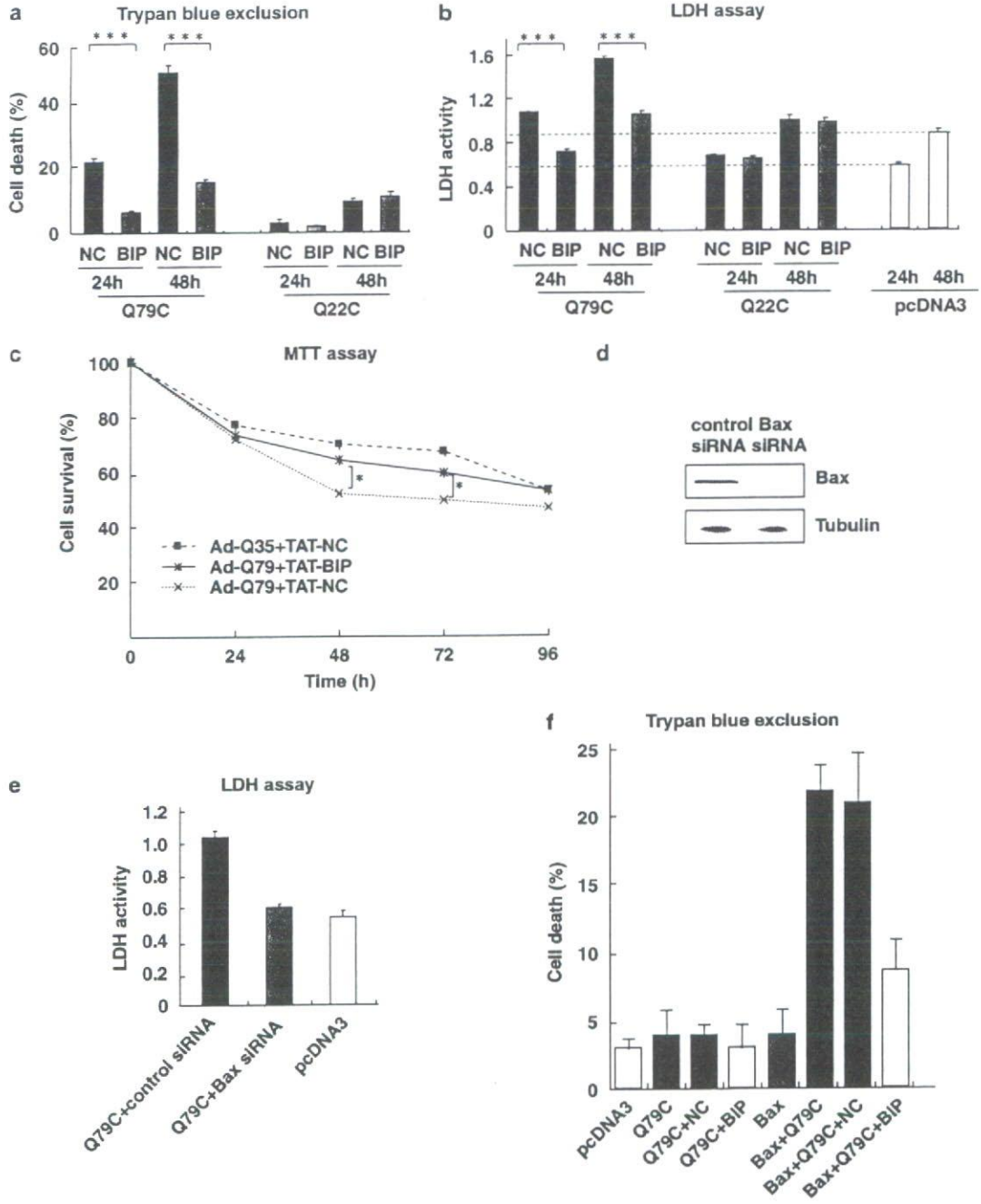

Figure 1 BIP suppresses Q79C-induced cell death. (**a** and **b**) Neuro-2a cells in 24-well plates were transfected with pCMX HA-Q22C (0.5 μg), pCMX HA-Q79C (0.5 μg) or pcDNA3 (0.5 μg) in the presence of 200 μM VPTLK (BIP) or negative control peptide (IPMIK; NC). Cell death was analyzed by Trypan blue exclusion (**a**) or LDH release into the medium (**b**) at both 24 and 48 h after transfection; ***$P<0.001$. (**c**) Primary cortical neurons in 24-well plates were infected with Ad-Q79C or Ad-Q35C at m.o.i. 100 in the presence of 80 μM TAT-VPTLK (TAT-BIP) or negative control peptide (TAT-IPMIK; TAT-NC). Cell death was analyzed by MTT assay at 24, 48, 72 and 96 h after treatment. The relative number of surviving cells was determined in triplicate by estimating the value of unstimulated or uninfected cells as 100%; *$P<0.05$. (**d** and **e**) The Bax siRNA suppresses Q79C toxicity. HEK293T cells in 24-well plates were transfected with pCMX HA-Q79C (0.5 μg) and 100 nM of control siRNA or Bax siRNA. The suppression of endogenous Bax expression by Bax siRNA was confirmed by Western blotting (**d**). The effect of Bax siRNA on Q79C-induced cell death is shown (**e**). (**f**) DU145 cells (Bax-deficient cells) in six-well plates were transfected with pcDNA3 (1 μg), pCMX HA-Q79C (1 μg) or pcDNA3-Bax (0.25 μg), and were cultured in the presence or absence of 200 μM VPMLK (BIP) or negative control peptide (IPMIK; NC). Cell death was analyzed by Trypan blue exclusion at 48 h after transfection

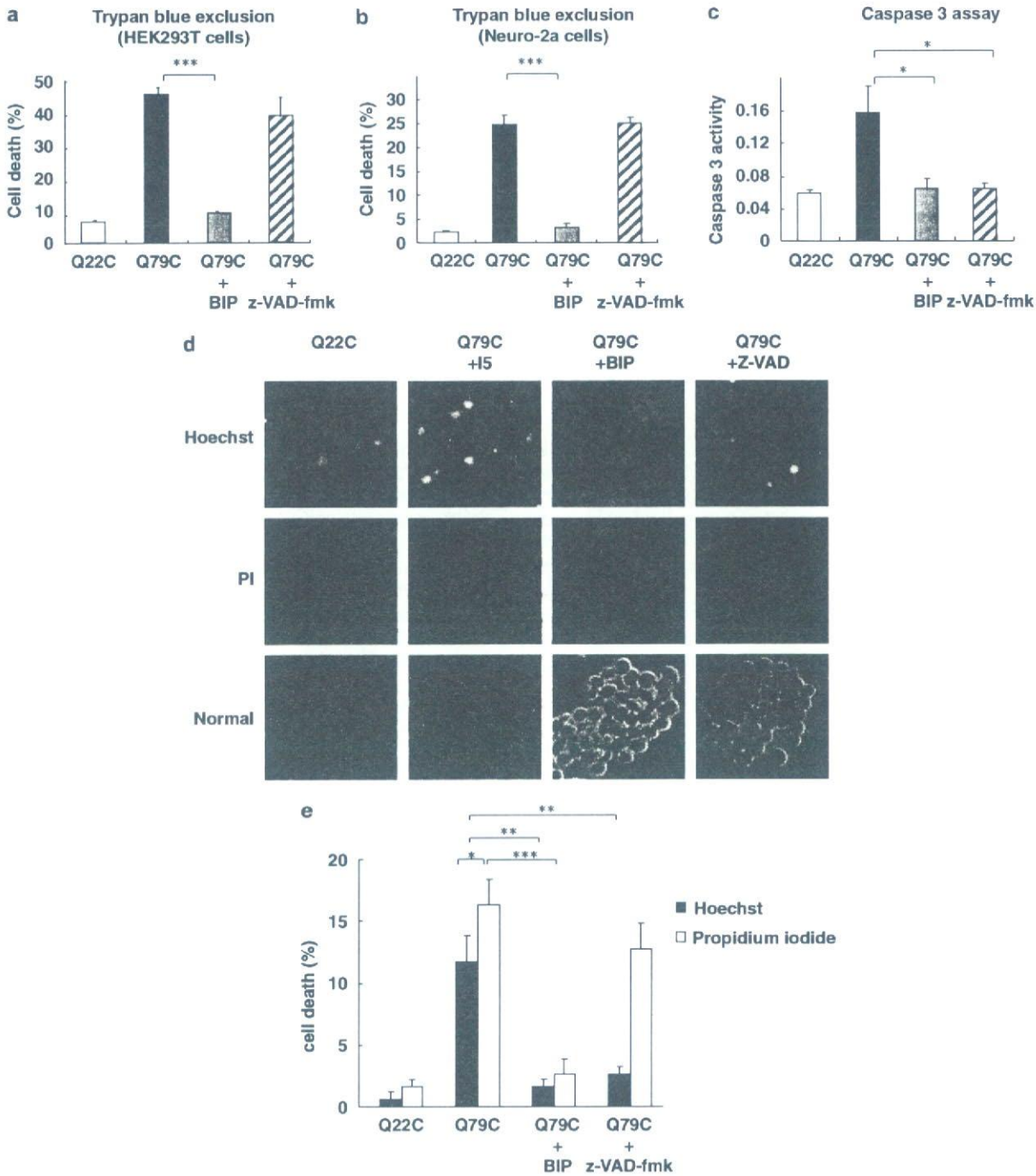

Figure 2 BIP suppresses both caspase-dependent and -independent cell death induced by Q79C. (**a**–**c**) HEK293T (**a**) or Neuro-2a cells (**b** and **c**) in 24-well plates were transfected with pCMX HA-Q22C (0.5 μg) or pCMX HA-Q79C (0.5 μg) in the presence of 200 μM VPMLK (BIP) or 100 μM of caspase inhibitor (z-VAD-fmk). At 48 h after transfection, cell death was determined by Trypan blue exclusion (**a** and **b**), and apoptotic events were evaluated by caspase 3 activity (**c**) $^{*}P<0.05$ or $^{***}P<0.001$. (**d** and **e**) Neuro-2a cells in 24-well plates were transfected with pCMX HA-Q22C (0.5 μg) or pCMX HA-Q79C (0.5 μg) in the presence of 200 μM VPMLK (BIP) or 100 μM of caspase inhibitor (z-VAD-fmk). At 48 h after transfection, cell death was determined by double staining with Hoechst (**d**, upper panel). PI (**d**, middle panel) and normal light field image (**d**, lower panel). The percentages of apoptotic cells with nuclear condensation and fragmentation and dead cells detected by PI staining (membrane integrity loss) are presented. Results are shown as mean $\pm$ S.E. of triplicated samples

The siRNA significantly inhibited Q79C-induced cell death (Figure 1e). Furthermore, we examined the cytotoxicity of polyQ in a Bax-deficient cell line, DU145 (human prostate cancer cell line).[18] Q79C did not show significant toxicity in DU145 cells, although Q79C induced cell death if Bax expression was restored (Figure 1f). These results suggest that Bax is a key mediator of Q79C-induced cell death.

BIP suppresses Q79C-induced nuclear fragmentation and cytoplasmic vacuolation. Next, we examined the effect of a pan-caspase inhibitor on Q79C-induced cell death, because Bax activates the caspases resulting in apoptosis.[6] Unexpectedly, the pan-caspase inhibitor, z-VAD-fmk, did not show a significant cytoprotective effect against Q79C toxicity when cellular viability was examined by Trypan blue exclusion (Figure 2a and b) and lactate dehydrogenase (LDH) release from the cells into the medium (data not shown). To further determine the role of caspase in Q79C-induced cell death, we examined the increase in caspase activity and the occurrence of nuclear fragmentation. We found that Q79C induced caspase activation (Figure 2c) and nuclear fragmentation (Figure 2d and e), both of which could be attenuated by both inhibitors of Bax (BIP) and of caspases (z-VAD-fmk). Of note, the number of apoptotic cells detected by the presence of nuclear fragmentation (Figure 2d and e) was less than the net number of dead cells detected by staining of Trypan blue (Figure 2b) and propidium iodide (PI) (Figure 2d and e), suggesting that Q79C activates both caspase-dependent and -independent cell death pathways.

PolyQ-induced cell death is associated with an increased number of enlarged vacuoles.[19–21] We also found that Neuro-2a cells with Q79C expression showed marked cytoplasmic vacuolation. BIP suppressed cytoplasmic vacuolation (Figure 3a and b), whereas the caspase inhibitor did not. These results suggest that Q79C-induced vacuolation is Bax-dependent and caspase-independent. Collectively, BIP suppressed both caspase-dependent nuclear fragmentation and caspase-independent cytoplasmic vacuolation elicited by polyQ.

Q79C expression induces Ku70 acetylation that releases Bax from Ku70. Because BIP is designed from Ku70 which prevents Bax-mediated cell death,[8–10] we examined whether Q79C had any influence on the binding between Ku70 and Bax. Q79C significantly decreased the interaction between Bax and Ku70 (Figure 4a and b). Furthermore, we found that Q79C induced significant acetylation of Ku70 (Figure 4c). To be noted, the acetylation of Ku70 is known to dissociate Bax and Ku70.[12] Two lysine (K) residues in Ku70, K539 and K542, are critical acetylation sites that influence Ku70-Bax binding.[12] To test whether Ku70 acetylation plays a role for the activation of Bax by polyQ, we generated acetylation-resistant mutants of Ku70 and acetylation-mimicking mutants of Ku70 by substituting K539 and K542 with arginine (R) or glutamine (Q), respectively. Acetylation-resistant Ku70 mutants (K539R and K542R)[12] suppressed Q79C-induced cell death more efficiently than wild-type Ku70 (Figure 4d). In contrast, the acetylation-mimicking Ku70 mutants (K539Q and K542Q),[12] could not suppress Q79C-induced cell death. The expression of these Ku70 mutants alone did not affect the cell viability. These results support the hypothesis that Q79C expression activates Bax, at least in part, through Ku70 acetylation.

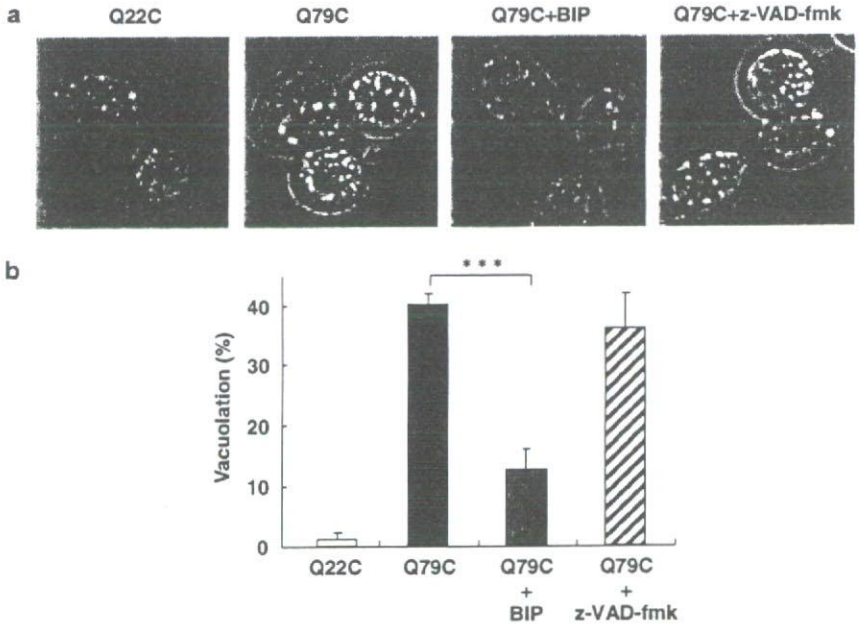

Figure 3 BIP suppresses Q79C-induced cytoplasmic vacuolation. Neuro-2a cells were transfected with pCMX HA-Q22C (0.5 μg) or pCMX HA-Q79C (0.5 μg) in the presence of 200 μM VPTLK (BIP) or 100 μM z-VAD-fmk. (**a**) At 48 h after transfection, the percent of cells with cytoplasmic vacuolation to all living cells were evaluated under optical microscopy ($\times$ 400); (**b**) ***$P<0.001$

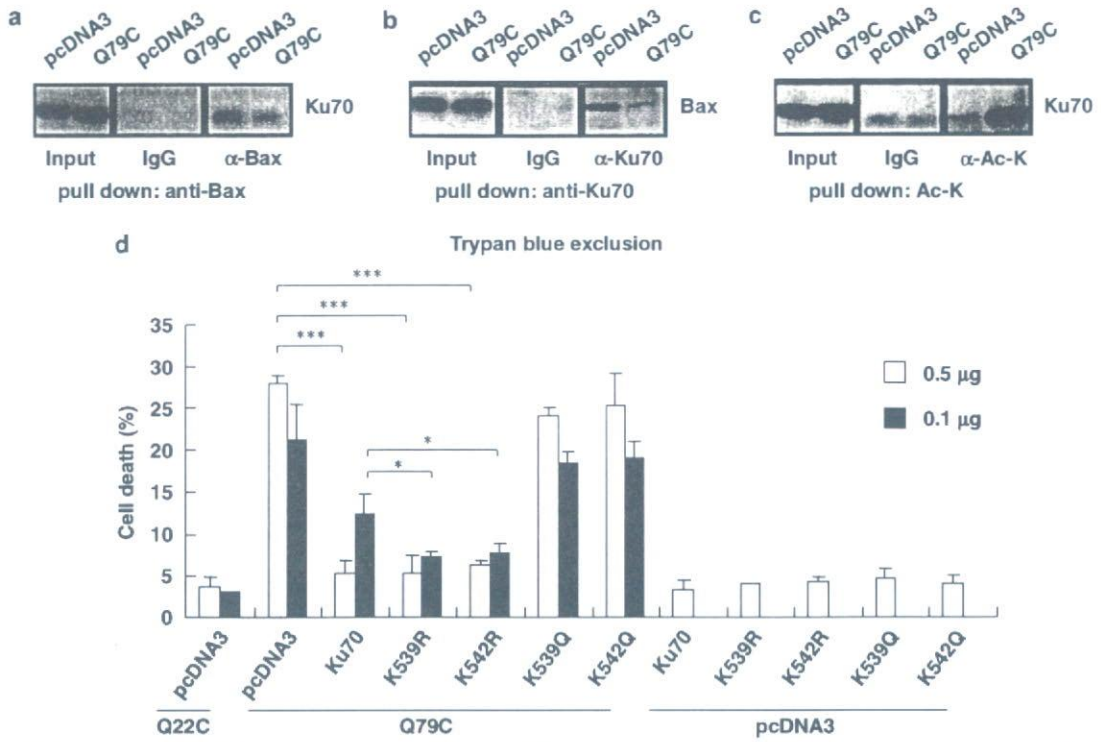

Figure 4 Q79C expression induces Ku70 acetylation that releases Bax from Ku70. (**a** and **b**) HEK293T cells in 10-cm dishes were transfected with pcDNA3 (10 μg) or pCMX HA-Q79C (10 μg). At 48 h after transfection, cells were harvested and immunoprecipitation was performed using anti-Bax (**a**) and anti-Ku70 monoclonal antibodies (**b**). Normal mouse IgG (IgG) was used as a negative control. Western blotting was performed with anti-Ku70 (**a**) or anti-Bax polyclonal (**b**) antibody. (**c**) HEK293T cells in 10-cm dishes were transfected with pcDNA3 (10 μg) or pCMX HA-Q79C (10 μg). After 48 h, cells were harvested and immunoprecipitation was performed using anti-pan-acetyl-lysine monoclonal antibody, and the acetylated Ku70 was detected by Western blotting with anti-Ku70 polyclonal antibody. (**d**) Neuro-2a cells in 24-well plates were co-transfected with pCMX HA-Q79C/Q22C (0.5 μg) and pcDNA3 (0.1 μg or 0.5 μg), wild-type Ku70 (0.1 μg or 0.5 μg) or Ku70 mutants (0.1 μg or 0.5 μg) bearing K→R (acetylation-resistant mutation) or K→Q substitutions (mutation that mimics acetylation) at positions K539 and K542. Cell death was analyzed by Trypan blue exclusion (**d**) at 48 h after transfection; $^{***}P<0.001$ or $^{*}P<0.05$

Ku70 and BIP inhibit Bax conformational change induced by polyQ expression. In cells with apoptotic stimuli, Bax is known to change its conformation, and the conformational change can be detected using the 6A7 anti-Bax monoclonal antibody that recognizes the N-terminus of Bax by immunoprecipitation.[22,23] The N-terminus exposure is an early step of Bax activation that occurs in the cytosol, and this conformational change is considered a prerequisite for membrane insertion of Bax at mitochondria and multimerization of Bax.[22–24] We found that Ku70 wild type and acetylation-resistant Ku70 (Ku70(K539R)), but not acetylation-mimicking Ku70 mutant (Ku70(K539Q)), inhibited the conformational change that was induced by polyQ expression (Figure 5a and b). It was also confirmed that BIP treatment significantly blocked Bax conformational change (Figure 5c). These results further support our hypothesis that Ku70 as well as BIP protect cells from polyQ toxicity by inhibiting Bax-mediated cell death.

Q79C binds Ku70 and histone acetyl transferase. Next, we examined how Q79C expression results in the acetylation of Ku70. The cyclic-AMP response element-binding protein (CBP) has been shown to acetylate cytosolic Ku70 in response to apoptotic stimuli.[12] Q79C is known to bind CBP in the nucleus.[4] We found that this interaction occurs in the cytosol too. We performed co-immunoprecipitation of polyQ and CBP using the cytosolic fraction and found that CBP was co-immunoprecipitated with Q79C, but not with Q22C (Figure 6a). In addition, we found that Ku70 binds both Q79C and Q22C in the cytosolic fraction (Figure 6b). We further confirmed the interaction of Q79C and CBP in the cytosol fraction (Figure 6c). These results suggest that Q79C stimulates Ku70 acetylation by bridging Ku70 and CBP (Figure 6d).

SIRT1 deacetylase and resveratrol rescue Q79C-induced cell death. The significant role of Ku70 acetylation in Q79C-induced cell death implies the possibility that the stimulation of deacetylases could reduce the polyQ toxicity. First, we examined the effect of the SIRT1 deacetylase, which has been demonstrated to deacetylate Ku70.[12] Overexpression of SIRT1 suppressed Q79C-induced cell death in Neuro-2a cells (Figure 7a and b). Small polyphenolic molecules such as resveratrol have been found to increase the affinity of SIRT1 and its target proteins.[25] We found that resveratrol markedly suppressed the cell death induced by Q79C in the HEK293T cells and primary cortical neurons (Figure 7c–e). We confirmed that SIRT1expression and resveratrol

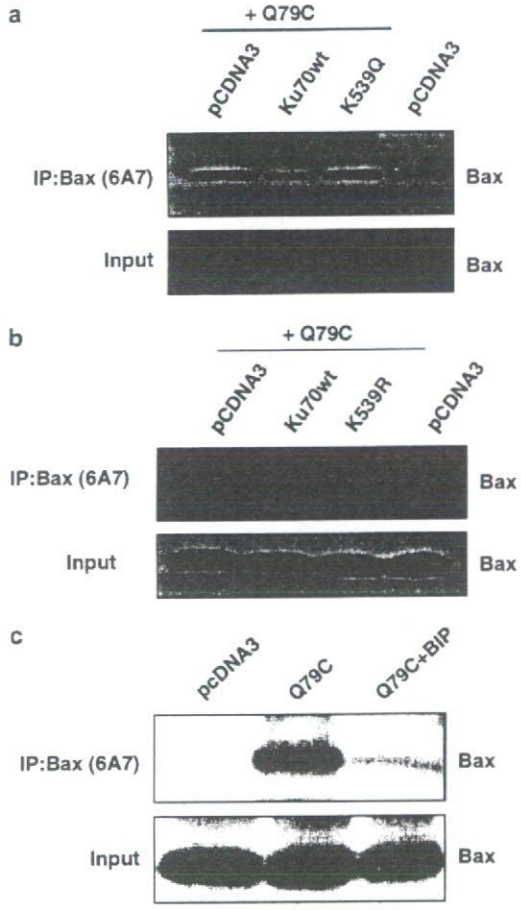

Figure 5 Ku70 and BIP inhibit Bax conformational change induced by polyQ expression. (**a** and **b**) Ku70 inhibits conformational change of Bax induced by Q79C. Neuro2a cells in 10-cm dishes were transfected with pcDNA3 (5 μg) or pCMX HA-Q79C (5 μg) together with pCMV-2B-Ku70 (5 μg), K539Q (acetylation-mimicking mutant) (5 μg) or K539R (acetylation-resistant mutant). After 48 h, cells were harvested and immunoprecipitation was performed using 6A7 anti-Bax monoclonal antibody. (**c**) HEK293T cells in 10-cm dishes were transfected with pcDNA3 (10 μg) or pCMX HA-Q79C (10 μg) in the presence or absence of 200 μM VPMLK (BIP). After 48 h, cells were harvested and immunoprecipitation was performed using 6A7 anti-Bax monoclonal antibody

treatment reduced the acetylation levels of Ku70 that was increased by Q79C expression (Figure 7f).

Discussion

We demonstrated that the inhibition of Bax by Ku70 and BIP markedly protected cells from polyQ toxicity. These results indicate that Bax plays a key role in polyQ toxicity. Our data also suggest that polyQ expression activates two different pathways of cell death. One is caspase-dependent cell death associated with nuclear fragmentation, and the other is caspase-independent cell death associated with cytoplasmic vacuolation, both of which were dramatically decreased by BIP. Cytoplasmic vacuolation has been observed in the neurons of patients with polyQ diseases.[19–21] Importantly, Bax is known to induce both caspase-independent and -dependent cell death with cytoplasmic vacuolation when caspase activity is inhibited or absent.[26–28] These previous reports support our hypothesis that Bax is a key mediator of Q79C-induced cell death associated with cytoplasmic vacuolation. Recently, an elevated expression of Bax was reported in the brain of polyQ-transgenic mouse.[29,30] We also observed that the number of pontine nucleus and microglia stained by anti-Bax 6A7-Ab in the brain section of MJD patient was significantly higher than those of normal controls (Supplementary Figure 3). Although this result is consistent with our findings in cell culture system, there are potential limitations of such experiments using human tissue, as the conditions and timing of specimen collection cannot be strictly controlled. Further extensive investigation is needed to determine the role of Bax in MJD pathogenesis in patient brain.

The significant ability of BIP to suppress Q79C-induced cell death suggests the possibility that Q79C expression causes dissociation of Ku70 from Bax. Previously, we reported that apoptotic stimuli decreased cytosolic levels of Ku70, and that this change may be one of the mechanisms for Ku70 dissociation from Bax.[31] However, in the case of Q79C expression, the decrease of Ku70 levels was not clear (Figure 4a and c, Ku70 input). The acetylation of Ku70 is known to be another mechanism releasing Bax from Ku70.[12] As shown in Figure 4, Q79C induced a significant acetylation of Ku70. We also confirmed that Ku70 mutants mimicking acetylation did not suppress Q79C-induced cell death, whereas acetylation-resistant Ku70 mutants rescued cells from Q79C toxicity more efficiently than Ku70 wild type. These results suggest that Ku70 acetylation is one of the major causes of Bax activation in Q79C-expressing cells.

SIRT1, one of the mammalian silent information regulator 2 (Sir2) homologues, was identified as a cell survival factor that protects cells from DNA damage.[32] SIRT1 was shown to have the activity to deacetylate several transcription factors, and through this activity, SIRT1 regulates a wide array of cellular processes for cell defense and survival under various stress conditions (reviewed by Baur and Sinclair[25]). Recently, resveratrol, an activator of the Sir2 histone deacetylase (HDAC),[25] has been reported to rescue polyQ-induced neuronal dysfunction in *Caenorhabditis elegans*.[33] Similarly, in the present study, SIRT1 deacetylase and resveratrol both effectively rescued cultured cells from polyQ toxicity. We confirmed that Ku70 was acetylated by Q79C and that Ku70 was deacetylated by resveratrol and SIRT1. These observations support our hypothesis that Ku70 acetylation plays an important role in Q79C-induced cell death.

It has been hypothesized that polyQ toxicity is caused by decreased histone acetylation, as polyQ sequesters histone acetyl transferase (HAT) (e.g. CBP) from chromosomes.[2,3] The subsequent suppression of histone acetylation decreases cellular transcriptional activities, and these changes are implicated to cause polyQ toxicity. Based on this hypothesis, the maintenance of histone acetylation by HDAC inhibitors, such as trichostatin A (TSA), has been examined for the reduction of polyQ toxicity.[3,34,35] However, an HDAC inhibitor was recently shown to induce apoptosis in neuroblastoma cells by increasing Ku70 acetylation and promoting Bax-mediated cell death.[14] Therefore, it is plausible that HDAC inhibitors have a 'double-edge' activity in the context of

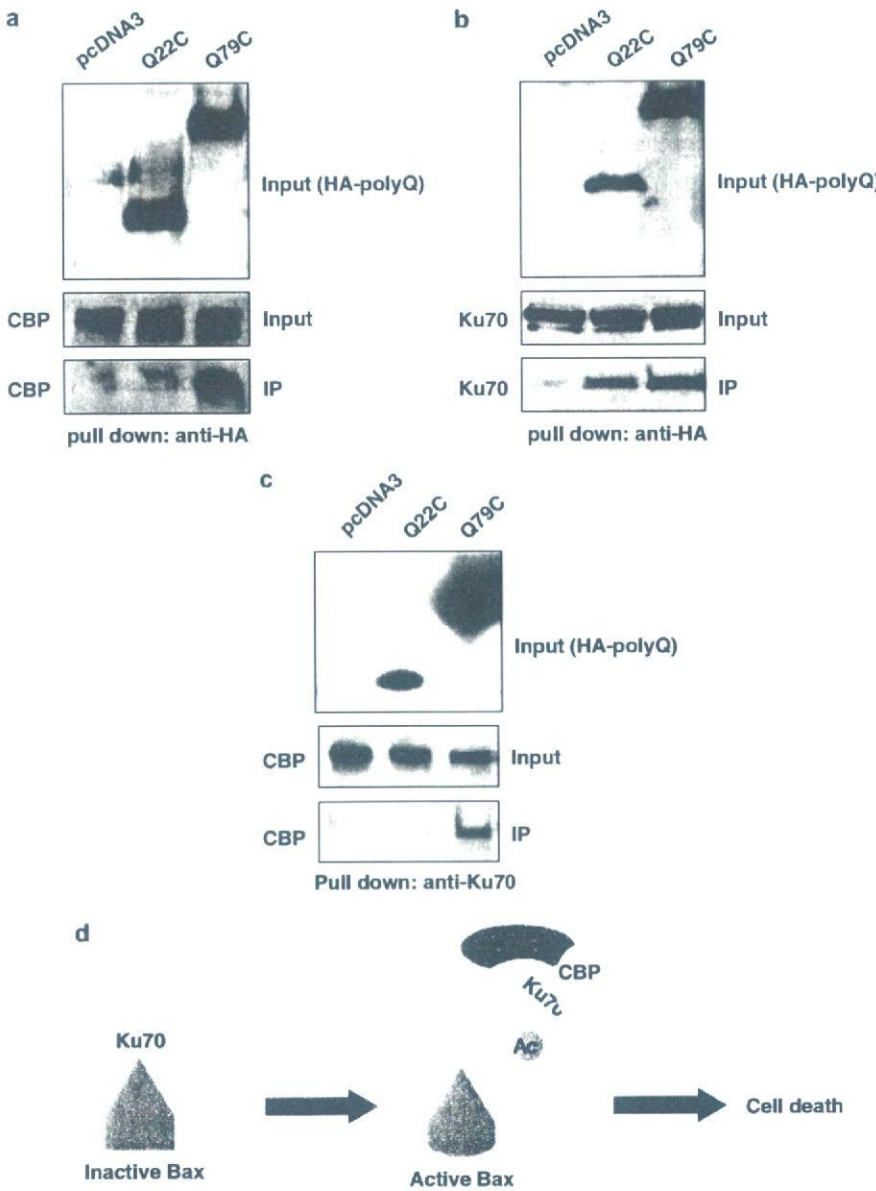

Figure 6 Q79C binds Ku70 and CBP. (**a**–**c**) HEK293T cells were transfected as described in Figure 4a and b, and the cytosolic fraction was used for immunoprecipitation. Immunoprecipitation was performed using anti-HA (**a** and **b**) or anti-Ku70 monoclonal antibody (**c**). Western blotting analyses of HA-tagged polyQ (Q22C and Q79C), CBP and Ku70 are shown. (**d**) Schematic representation of Bax activation by Ku70 acetylation during Q79C-induced cell death

polyQ toxicity; they attenuate polyQ toxicity by maintaining histone acetylation in the nucleus, but promote Bax-mediated cell death by acetylating Ku70 in the cytosol. In cultured cells, TSA can attenuate Q79C-induced cell death only at the lower doses (3–10 nM), whereas it enhances cell death at the higher doses (more than 20 nM) (Supplementary Figure 2). Actually, the therapeutic effect of an HDAC inhibitor was observed only within a narrow range of lower doses, and the effect changed to be toxic at higher doses in polyQ transgenic mice.[35] These results suggest that the use of HDAC inhibitors in polyQ diseases requires careful consideration to avoid causing a lethal degree of Ku70 acetylation. The present study focused on the toxicity of expanded polyQ derived from the causative gene (mutated ataxin3) of MJD. Thus, further study is needed to examine whether our observation can be generally confirmed in other types of toxic polyQ such as that of Huntington's disease and spinocerebellar ataxia type 1 (SCA1).

In conclusion, we propose that Bax is a key mediator of Q79C-induced cell death and that Bax activation is mediated through acetylation of Ku70, which dissociates Bax from Ku70. Our hypothesis is based on the observation in cell culture studies, and further extensive studies using *in vivo* models are clearly needed. The present study suggests that

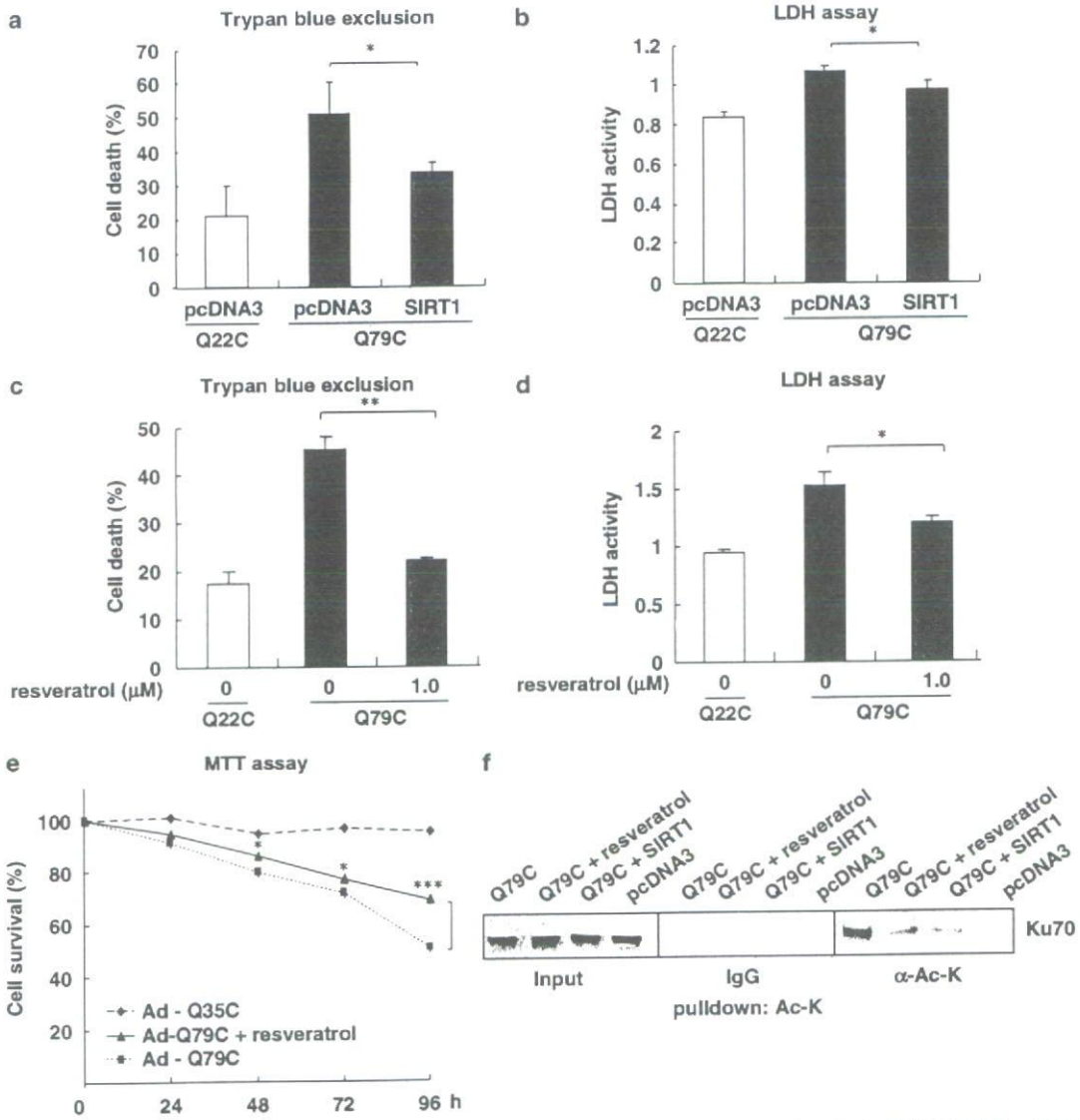

Figure 7 Effects of SIRT1 and resveratrol on Q79C-induced cell death. Neuro-2a cells in 24-well plates were co-transfected with pCMX HA-Q79C or -Q22C (0.5 μg) and pcDNA3 (0.5 μg), or pcDNA3-SIRT1 (0.5 μg). Cell death was analyzed by Trypan blue exclusion (**a**) or LDH release into the medium (**b**) at 48 h after transfection; $^{*}P<0.05$. HEK293T cells in 24-well plates were transfected with pCMX HA-Q79C (0.5 μg) or pCMX HA-Q22C (0.5 μg) in the presence of resveratrol (1 μM). Cell death was assessed by Trypan blue exclusion (**c**) or LDH release into the medium (**d**) at 72 h after transfection; $^{**}P<0.01$ or $^{*}P<0.05$. (**e**) Primary cortical neurons in 24-well plates were infected with Ad-Q79C or Ad-Q35C at m.o.i. 100 in the presence of resveratrol (1 μM). Cell death was analyzed by MTT assay at 24, 48, 72 and 96 h after treatment. The relative number of surviving cells was determined in triplicate by estimating the value of unstimulated or uninfected cells as 100%; $^{***}P<0.001$ or $^{*}P<0.05$. (**f**) HEK293T cells in 10-cm dishes were transfected with pCMX HA-Q79C (5 μg) and pcDNA3-SIRT1 (5 μg), or with pCMX HA-Q79C (5 μg) in the presence of resveratrol (1 μM). After 48 h, cells were harvested and immunoprecipitation was performed using anti-pan-acetyl-lysine monoclonal antibody. The acetylated Ku70 was detected by Western blotting with anti-Ku70 polyclonal antibody

the inhibition of Bax by BIPs or Ku70 may provide a new strategy to develop therapeutics for MJD.

Materials and Methods

Plasmid constructs and recombinant adenoviruses. The expression plasmids of ataxin-3 were kindly given Dr. Akira Kakizuka. The MJD1 cDNA in the plasmid was a truncated fragment including either 22 (normal, pCMX HA-Q22C) or 79 (expanded, pCMX HA-Q79C) repeats of CAG, and was hemagglutinin (HA)-fused on the N-terminus. The plasmids, pcDNA3-Bax and pCMV 2B-Flag-Ku70 have been described previously.[12] pCMV 2B-Flag-Ku70 K539R/K542R/K539Q/K542Q were generated by QuickChange Site-Directed Mutagenesis Kit from Stratagene. SIRT1 expression plasmid was generated by subcloning the coding sequence of SIRT1 cDNA (kindly provided by Dr. Shinichirou Imai) into the pcDNA3 vector (Invitrogen). Recombinant adenoviruses encoding Flag-Q79C and Flag-Q35C were constructed as described previously.[36]

Cell culture and transfection. HEK293T, Neuro-2a and DU145 cells were cultured in DMEM containing 10% fetal bovine serum. Transfection of plasmids was

performed with Lipofectamine Plus reagent (Invitrogen) in accordance with the manufacturer's instructions. For cell death analysis with HEK293T and Neuro-2a cells, transfection efficiency was monitored with co-transfected 50 ng of pEGFP-C2 (Clontech), and confirmed that the efficiency was more than 75% before analysis.

Rat primary cortical neurons. Cortices were dissected from E-18 Sprague-Dawley rats' brains. Rat cortical neurons were plated into poly-D-lysine-coated 24-well plates. Mixed cultures were maintained in neurobasal medium. After 72 h of culture, 10 mM of cytosine arabinoside (Ara-C) was added to stop the proliferation of glial cells. After 72 h of Ara-C-treated, medium was replaced with fresh neurobasal medium.

Cell death assays. Cell death was assessed by Trypan blue exclusion, PI exclusion, LDH relase, Hoechst dye nuclear staining, MTT assay and caspase activity measurement.

For Trypan blue exclusion test, cells were collected and centrifuged for 10 min at 1000 r.p.m. The cell pellet was resuspended in 50 μl of DMEM, to which 50 μl of Trypan blue (0.4%) was added. Dead cells were counted by three independent hemocytometer counts.

LDH release from the cells into the medium was analyzed by the Cytotox 96 nonradioactive cytotoxicity assay (Promega). Cell viability of primary cortical neurons was determined by MTT assay (Chemicon) and LDH release into the medium. Nuclear condensation and membrane integrity loss were monitored by observing cells under a fluorescence microscope after application of 1 μg/ml Hoechst dye 33258 and 4 μg/ml PI. Caspase 3 activities of cells were measured with Caspase 3 Assay Kit (Sigma) in accordance with the manufacturer's instructions. For each experiment, data were obtained from three wells.

Statistical analyses for cell death were performed using the student's *t*-test and single-factor ANOVA, followed by Fisher's protected least-significant difference *post hoc* test. The results were confirmed in more than three independent experiments of all cell death analysis and Western blottings.

siRNA preparation. Sense and antisense strands of siRNA oligonucleotides were synthesized, and were then annealed at 95°C for 1 min. The sense sequence of siRNA-Bax is 5′-CCAAGAAGCUGAGCGAGUGdTdT-3′ and the sequence of control siRNA is 5′-GGUCUCGUAGACCGUGCACdTdT-3′.

Immunoprecipitation. For detecting the active form of Bax (Figure 5a–c), transfected HEK293T cells in 10-cm dishes were lysed in 200 μl Chaps buffer (150 mM NaCl, 10 mM HEPES at pH 7.4 and 1.0% Chaps) containing the protease inhibitors (1 : 100 dilution of protease inhibitor Cocktail; Sigma), according to the previously reported methods.[22] After pre-clearing 200 μl of the sample with 20 μl protein A-sepharose (CL-4B, 17-0780-01; Amersham Biosciences) at 4°C for 1 h, immunoprecipitation was performed by incubating 200 μl of the lysates with 2 μg of anti-Bax monoclonal antibody (clone 6A7, BD-Pharmingen) at 4°C for 2 h. Immunocomplexes in 200 μl of the lysates were precipitated with 20 μl protein A-sepharose. After extensive washing with buffer, beads were boiled in 40 μl Laemmli buffer, and 20 μl of the eluted proteins were analyzed by Western blotting. Western blotting analysis of pre-immunoprecipitation (input) and immunoprecipitated samples (IP) were performed with an anti-Bax polyclonal antibody (N-20, sc-493; Santa Cruz).

For detecting Bax-Ku70 interactions (Figure 4a and b), transfected HEK293T cells in 10-cm dishes were lysed in 200 μl Chaps buffer containing the protease inhibitors. After pre-clearing 200 μl of the sample with 20 μl protein G-sepharose (4 Fast Flow, 17-0618-01; Amersham Biosciences) at 4°C for 1 h, immunoprecipitation was performed by incubating 200 μl of the lysates with 2 μg of monoclonal anti-Bax antibody (B9, Santa Cruz) or 2 μg of monoclonal anti-Ku70 antibody (A9, Santa Cruz) at 4°C for 2 h. Immunocomplexes in 200 μl of the lysates were precipitated with 20 μL protein G-sepharose. After extensive washing with buffer, beads were boiled in 40 μl Laemmli buffer, and 20 μl of the eluted proteins were analyzed by Western blotting. Mouse IgG was used as negative control. Western blotting analysis of pre-immunoprecipitation (input) and immunoprecipitated samples (α-Bax or α-Ku70) were performed with an anti-Ku70 polyclonal antibody (H-308, sc-9033; Santa Cruz) or an anti-Bax polyclonal antibody (N-20, sc-493; Santa Cruz).

For detecting the acetylated form of Ku70 (Figures 4c and 7f), transfected HEK293T cells in 10-cm dishes were lysed in 200 μl 1% triton in phosphate-buffered saline containing the protease inhibitors and 5 μM TSA (Sigma).[12] After pre-clearing 200 μl of the sample with 20 μl protein G-sepharose at 4°C for 1 h, immunoprecipitation was performed by incubating 200 μl of the lysates with 4 μg of anti-pan-acetyl-lysine monoclonal antibody (9681S; Cell Signaling) at 4°C for 2 h. Immunocomplexes in 200 μl of the lysates were precipitated with 20 μl protein G-sepharose. After extensive washing with buffer, beads were boiled in 40 μl Laemmli buffer, and 20 μl of the eluted proteins were analyzed by Western blotting. Mouse IgG was used as negative control. Western blotting analysis of pre-immunoprecipitation (input) and immunoprecipitated samples (α-Ac-K) were performed with an anti-Ku70 polyclonal antibody (H-308, sc-9033; Santa Cruz).

For detecting the interactions of HA-polyQ (Q79C) and CBP or Ku70, Ku70 and CBP (Figure 6a–c), transfected HEK293T cells in 10-cm dishes were homogenized with 350 μl of ice-cold homogenization buffer (250 mM sucrose, 20 mM HEPES at pH 8.0, 10 mM KCl, 1.5 mM $MgCl_2$, 1 mM EDTA, 1 mM EGTA, pH 7.5 and 0.1 mM PMSF) containing the protease inhibitors. The cytosolic fraction was prepared by collecting the supernatant of the centrifuged homogenate samples at 14 000 r.p.m. for 30 min at 4°C. Immunoprecipitation was performed by incubating 300 μl of the lysates with 40 μl of anti-HA antibody-conjugated beads (HA-7, A2095; Sigma) or with 2 μg anti-Ku70 monoclonal antibody (A-9, sc-5309; Santa Cruz) at 4°C for 2 h. Immunocomplexes of anti-Ku70 monoclonal antibody in 200 μl of the lysates were precipitated with 20 μl protein G-sepharose beads (4 Fast Flow, 17-0618-01; Amersham Biosciences). After extensive washing with buffer, beads were boiled in 40 μl Laemmli buffer, and 20 μl of the eluted proteins were analyzed by Western blotting. Western blotting analysis of pre-immunoprecipitation (input) and immunoprecipitated samples (IP) were performed with an anti-HA polyclonal antibody (HA-7, H9658; Sigma), anti-CBP polyclonal antibody (C-20, sc-583; Santa Cruz) or anti-Ku70 polyclonal antibody (H-308, sc-9033; Santa Cruz).

Acknowledgements. We thank Dr. Akira Kakizuka for providing ataxin-3-expressing plasmid, Dr. Hideki Nishitoh for recombinant adenoviruses encoding Q79C and Q35C, Dr. Shinichirou Imai for providing mouse SIRT1 cDNA and Dr. Hideki Mochizuki for providing mouse tissue sample treated with MPTP as positive control of activated Bax. We also thank Ms. Keiko Kaneko, Ms. Kanae Yonetsu and Ms. Iku Sudo for their technical help. This work was supported in part by a grant from the 21st Century COE Program on Brain Integration and its Disorders to Tokyo Medical and Dental University (to YL and HM), Japan Foundation for Neuroscience and Mental Health (to YL, TY and HM), National Institute of Health (USA) (P20CA10373 to SM) and American Heart Association (to VG (predoctoral fellowship), JG (predoctoral fellowship) and SM (Grant-in-Aid)).

1. Ross CA. Polyglutamine pathogenesis: emergence of unifying mechanisms for Huntington's disease and related disorders. *Neuron* 2002; **35**: 819–822.
2. Shimohata T, Nakajima Tm, Yamada M, Uchida C, Onodera O, Naruse S. Expanded polyglutamine stretches interact with TAFII130, interfering with CREB-dependent transcription. *Nat Genet* 2000; **26**: 29–36.
3. Steffan JS, Bodai L, Pallos J, Poelman M, McCampbell A, Apostol BL *et al.* Histone deacetylase inhibitors arrest polyglutamine-dependent neurodegeneration in *Drosophila*. *Nature* 2001; **413**: 739–743.
4. Li F, Macfarlan T, Pittman RN, Chakravarti D. Ataxin-3 is a histone-binding protein with two independent transcriptional corepressor activities. *J Biol Chem* 2002; **277**: 45004–45012.
5. Deckwerth TL, Elliott JL, Knudson CM, Johnson Jr EM, Snider WD, Korsmeyer SJ. BAX is required for neuronal death after trophic factor deprivation and during development. *Neuron* 1996; **17**: 401–411.
6. Vaux DL, Korsmeyer SJ. Cell death in development. *Cell* 1999; **96**: 245–254.
7. Bae BI, Xu H, Igarashi S, Fujimuro M, Agrawal N, Taya Y *et al.* p53 mediates cellular dysfunction and behavioral abnormalities in Huntington's disease. *Neuron* 2005; **47**: 29–41.
8. Yoshida T, Tomioka I, Nagahara T, Holyst T, Sawada M, Hayes P *et al.* Bax-inhibiting peptide derived from mouse and rat Ku70. *Biochem Biophys Res Commun* 2004; **321**: 961–966.
9. Gomez JA, Gama V, Matsuyama S. Cell-permeable penta-peptides derived from Bax-inhibiting peptide. *Handbook of Cell Penetrating Peptides*, 2nd edn., CRC Press: Ulo Langel, 2006, pp 469–481.
10. Gomez J, Gama V, Yoshida T, Sun W, Hayes P, Leskov K *et al.* Bax Inhibiting Peptides (BIPs) derived from Ku70 and Cell Penetrating Penta-Peptides (CPP5s). *Biochem Soc Trans* 2007; **35**: 797–801.
11. Downs JA, Jackson SP. A means to a DNA end: the many roles of Ku. *Nat Rev Mol Cell Biol* 2004; **5**: 367–378.
12. Cohen HY, Lavu S, Bitterman KJ, Hekking B, Imahiyerobo TA, Miller C *et al.* Acetylation of the C terminus of Ku70 by CBP and PCAF controls Bax-mediated apoptosis. *Mol Cell* 2004; **13**: 627–638.
13. Cohen HY, Miller C, Bitterman KJ, Wall NR, Hekking B, Kessler B *et al.* Calorie restriction promotes mammalian cell survival by inducing the SIRT1 deacetylase. *Science* 2004; **305**: 390–392.

14. Subramanian C, Opipari Jr AW, Bian X, Castle VP, Kwok RP. Ku70 acetylation mediates neuroblastoma cell death induced by histone deacetylase inhibitors. *Proc Natl Acad Sci USA* 2005; **102**: 4842–4847.
15. Ikeda H, Yamaguchi M, Sugai S, Aze Y, Narumiya S, Kakizuka A. Expanded polyglutamine in the Machado–Joseph disease protein induces cell death in vitro and *in vivo*. *Nat Genet* 1996; **13**: 196–202.
16. Nishitoh H, Matsuzawa A, Tobiume K, Saegusa K, Takeda K, Inoue K *et al*. ASK1 is essential for endoplasmic reticulum stress-induced neuronal cell death triggered by expanded polyglutamine repeats. *Genes Dev* 2002; **16**: 1345–1355.
17. Xia H, Mao Q, Davidson BL. The HIV Tat protein transduction domain improves the biodistribution of beta-glucuronidase expressed from recombinant viral vectors. *Nat Biotechnol* 2001; **19**: 640–644.
18. Rampino N, Yamamoto H, Ionov Y, Li Y, Sawai H, Reed JC *et al*. Somatic frameshift mutations in the BAX gene in colon cancers of the microsatellite mutator phenotype. *Science* 1997; **275**: 967–969.
19. Clark HB, Burright EN, Yunis WS, Larson S, Wilcox C, Hartman B *et al*. Purkinje cell expression of a mutant allele of SCA1 in transgenic mice leads to disparate effects on motor behaviors, followed by a progressive cerebellar dysfunction and histological alterations. *J Neurosci* 1997; **17**: 7385–7395.
20. Sapp E, Schwarz C, Chase K, Bhide PG, Young AB, Penney J *et al*. Huntingtin localization in brains of normal and Huntington's disease patients. *Ann Neurol* 1997; **42**: 604–612.
21. Hirabayashi M, Inoue K, Tanaka K, Nakadate K, Ohsawa Y, Kamei Y *et al*. VCP/p97 in abnormal protein aggregates, cytoplasmic vacuoles, and cell death, phenotypes relevant to neurodegeneration. *Cell Death Differ* 2001; **8**: 977–984.
22. Hsu YT, Youle RJ. Bax in murine thymus is a soluble monomeric protein that displays differential detergent-induced conformations. *J Biol Chem* 1998; **273**: 10777–10783.
23. Nechushtan A, Smith CL, Hsu YT, Youle RJ. Conformation of the Bax C-terminus regulates subcellular location and cell death. *EMBO J* 1999; **18**: 2330–2341.
24. Upton JP, Valentijn AJ, Zhang L, Gilmore AP. The N-terminal conformation of Bax regulates cell commitment to apoptosis. *Cell Death Differ* 2007; **14**: 932–942.
25. Baur JA, Sinclair DA. Therapeutic potential of resveratrol: the *in vivo* evidence. *Nat Rev Drug Discov* 2006; **5**: 493–506.
26. Xiang J, Chao DT, Korsmeyer SJ. BAX-induced cell death may not require interleukin 1 beta-converting enzyme-like proteases. *Proc Natl Acad Sci USA* 1996; **93**: 14559–14563.
27. Zha H, Fisk HA, Yaffe MP, Mahajan N, Herman B, Reed JC. Structure-function comparisons of the proapoptotic protein Bax in yeast and mammalian cells. *Mol Cell Biol* 16; **1996**: 6494–6508.
28. Jurgensmeier JM, Krajewski S, Armstrong RC, Wilson GM, Oltersdorf T, Fritz LC *et al*. Bax- and Bak-induced cell death in the fission yeast *Schizosaccharomyces pombe*. *Mol Biol Cell* 1997; **8**: 325–339.
29. Chou AH, Yeh TH, Kuo YL, Kao YC, Jou MJ, Hsu CY *et al*. Polyglutamine-expanded ataxin-3 activates mitochondrial apoptotic pathway by upregulating Bax and downregulating Bcl-xL. *Neurobiol Dis* 2006; **21**: 333–345.
30. Wang HL, He CY, Chou AH, Yeh TH, Chen YL, Li AH. Polyglutamine-expanded ataxin-7 activates mitochondrial apoptotic pathway of cerebellar neurons by upregulating Bax and downregulating Bcl-x(L). *Cell Signal* 2006; **18**: 541–552.
31. Gama V, Yoshida T, Gomez JA, Basile DP, Mayo LD, Haas AL *et al*. Involvement of the ubiquitin pathway in decreasing Ku70 levels in response to drug-induced apoptosis. *Exp Cell Res* 2006; **312**: 488–499.
32. Imai S, Armstrong CM, Kaeberlein M, Guarente L. Transcriptional silencing and longevity protein Sir2 is an NAD-dependent histone deacetylase. *Nature* 2000; **403**: 795–800.
33. Parker JA, Arango M, Abderrahmane S, Lambert E, Tourette C, Catoire H *et al*. Resveratrol rescues mutant polyglutamine cytotoxicity in nematode and mammalian neurons. *Nat Genet* 2005; **37**: 349–350.
34. McCampbell A, Taye AA, Whitty L, Penney E, Steffan JS, Fischbeck KH. Histone deacetylase inhibitors reduce polyglutamine toxicity. *Proc Natl Acad Sci USA* 2001; **98**: 15179–15184.
35. Minamiyama M, Katsuno M, Adachi H, Waza M, Sang C, Kobayashi Y *et al*. Sodium butyrate ameliorates phenotypic expression in a transgenic mouse model of spinal and bulbar muscular atrophy. *Hum Mol Genet* 2004; **13**: 1183–1192.
36. Saitoh M, Nishitoh H, Fujii M, Takeda K, Tobiume K, Sawada Y *et al*. Mammalian thioredoxin is a direct inhibitor of apoptosis signal-regulating kinase (ASK) 1. *EMBO J* 1998; **17**: 2596–2606.

Supplementary Information accompanies the paper on Cell Death and Differentiation website (http://www.nature.com/cdd)

Research Signpost
37/661 (2), Fort P.O., Trivandrum-695 023, Kerala, India

Research Advances in Spinocerebellar Degeneration and Spastic Paraplegia, 2008: 57-68
ISBN: 978-81-308-0233-6 Editors: Yoshihisa Takiyama and Masatoyo Nishizawa

5

Chromosome 16q22.1-linked autosomal dominant cerebellar ataxia and spinocerebellar ataxia type 4, the two clinically distinct ataxias linked to the same locus

Kinya Ishikawa[1], Kevin Flanigan[2] and Hidehiro Mizusawa[3]
[1]Senior Assistant Professor and [3]Professor and Chairman, Department of Neurology and Neurological Sciences, Graduate School, Tokyo Medical and Dental University, Yushima 1-5-45, Bunkyo-ku 113-8519, Tokyo, Japan
[2]Associate Professor, Departments of Neurology and Human Genetics University of Utah, Salt Lake City, Utah, USA

Abstract

Autosomal dominant cerebellar ataxia (ADCA) is a group of neurodegenerative disorders inherited in autosomal dominant fashion. Although it is widely accepted that ADCA is heterogeneous both clinically

Correspondence/Reprint request: Dr. Kinya Ishikawa, Senior Assistant Professor, Department of Neurology and Neurological Sciences, Graduate School, Tokyo Medical and Dental University, Yushima 1-5-45, Bunkyo-ku 113-8519, Tokyo, Japan. E-mail: kishikawa.nuro@tmd.ac.jp

and genetically, varieties of clinical features seen in one given disorder could be explained by a combination of some clinical hallmarks which may clinically characterize the disorder. Here we describe spinocerebellar ataxia type 4 (SCA4) and chromosome 16q22.1-linked ADCA, the two distinct disorders linked to the same chromosomal region. Patients with spinocerebellar ataxia type 4 always show prominent sensory axonal neuropathy as well as cerebellar ataxia, while patients with 16q22.1-linked ADCA show isolated cerebellar ataxia with much later age of onset than SCA4. The two disorders also appear distinct neuropathologically: multiple system degenerations in SCA4 versus cerebellar cortical degeneration in 16q22.1-linked ADCA. A single-nucleotide change (-16C>T) in the puratrophin-1 gene, strongly associated with 16q22.1-linked ADCA, has not been seen in SCA4. Interestingly, the two disorders are limited so far in ethnically distinct populations: Scandinavians for SCA4 and Japanese for 16q22.1-linked ADCA. Are these two disorders allelic? Identification of causative gene(s) will ultimately settle this issue.

1. Introduction

Autosomal dominant cerebellar ataxia (ADCA) is a group of disorders with clinically and genetically heterogeneous conditions. As covered in this book, ADCA is divided in more than 30 disorders. Yet, the number of diseases comprising ADCA is expected to increase by identification of new responsible genes or gene loci.

In this chapter, we cover two ADCAs known to link to a small region in chromosome 16q22.1. The two disorders are, spinocerebellar ataxia type 4 (SCA4), and chromosome 16q22.1-linked ADCA. We first describe SCA4, and then 16q22.1-linked ADCA, as the order of disease identification. Finally, we describe recent progress on the pathogenesis of these disorders.

2. Spinocerebellar ataxia type 4 (SCA4)

In 1994, K. Gardner, L.J. Ptáček and their colleagues reported a five-generation family with ADCA, and showed a linkage to chromosome 16q13 (Gardner K. et al. 1994) [1]. Since this gene locus was the forth one responsible for ADCA, this family was named "spinocerebellar ataxia type 4 (SCA4)". Following their initial report, they examined a larger number of members in the same family, and refined the gene locus to a 6-cM (centi Morgan) region in the chromosome 16q22.1 [2]. These two reports are the original reports of SCA4 based on a single family.

This family resided in Utah and Wyoming in USA. They originated from Scandinavia. Clinically, the SCA4 family showed cerebellar ataxia of variable onset (19-59 years), with a mean age of onset at 39.3 years. In addition to cerebellar ataxia, the family was characterized by a distinct features compared

Table 1. A comparison of clinical features in SCA4 and 16q22.1-linked ADCA families.

	SCA4	SCA4	16q22.1-ADCA
Reference	#2	#3	
Ethnicity	American	German	Japanese
Number of patients	20	14	120
Age of onset (yrs)			
Ataxia	39.3	38.3	61.2
Hearing impairment	unknown	unknown	66.4
Frequencies of clinical signs and symptoms			
gait ataxia	95%	100%	100%
limb ataxia	95%	100%	92.6%
cerebellar speech	50.0%	100%	92.6%
nystagmus		57%	55%
muscle tonus			
normal			42.9%
reduced			57.1%
increased			0%
tendon reflex			
normal			71.4%
increased			0%
reduced			28.6%
absent	100%		0%
Babinski's sign	20%	7%	0%
tremor			14.3%
decreased vibratory sense	100%	100%	5.0%
loss of sensory nerve action potential	92.3%	100%	0%
dementia			0%
hearing impairment			42.7%

to other ADCAs. Among 20 affected individuals clinically examined, not only cerebellar ataxia, but also prominent sensory neuropathy was seen in nearly all patients [2]. Vibratory and joint-position senses were lost in all patients (100%), and pinprick sensation was also decreased in 95% of patients (Table 1). Ankle tendon reflexes were always absent, and 85% of patients also lacked reflexes in their knees. Complete areflexia was seen in 25% of patients. Sural sensory-nerve action potentials were absent in 12 out of 13 patients examined.

In addition to sensory neuropathy, dysarthria was noted in 50% of patients, and Babinski signs and distal weakness were both seen in 20% of patients. Eye movement were normal in most patients, except that slightly saccadic visual pursuit was noted in only two patients, and occasional spontaneous lateral movements with visual fixation was noted in one patient. Since previously known ADCAs commonly showed ophthalmoparesis as well as pyramidal & extrapyramidal tract signs as additional neurological features, prominent sensory disturbance with essentially normal eye movements in SCA4 appeared a very distinct combination. From a clinical standpoint, authors speculated that the main sites of degeneration should be the cerebellum and the dorsal root ganglia.

One of us (KF) and his colleagues [2] also performed fine mapping of the responsible gene by typing 5 microsatellite markers in chromosome 16q, and found that the disease in this family is tightly linked to a microsatellite marker D16S397, with a maximum two-point lod score of 5.93 at recombination (θ)=0. They also undertook detailed clinical investigation insights, and observed some family members with decreased sural nerve action potential without symptoms of sensory loss. This may indicate that subclinical neuropathy may be the earliest sign of SCA4.

The original Utah-Wyoming kindred had been the only SCA4 family known for a long time, until the second SCA4 family was identified from northern Germany in 2003 [3]. This German family also originated from Scandinavia (author's personal communication). The mean age of onset was at 38.3 $\pm$ 13.4 years, and the main clinical feature was cerebellar ataxia with prominent sensory neuropathy as in the Utah/Wyoming SCA4 family (Table 1). Of note is that, while sural nerve action potential was absent in all patients examined, reduced compound muscle action potential (CMAP) amplitude was seen in 3 out of 8 patients examined. This would indicate that motor axons are also affected in SCA4.

Since no other SCA4 families are known to date, presence of two families originated in the same area would indicate a founder effect.

Hellenbroich and others also mapped to their family around D16S397. By haplotype analysis, they observed two obligate recombinations, setting the centromeric border at D16S3019. Although telomeric recombination was not documented in their family, it was seen at D16S512 in the Utah/Wyoming

family [2]. These observations would indicate that the SCA4 gene lie in a 3.69 cM interval between D16S3019 and D16S512. This region is now considered 7.9 mega-base pair (Mb) in size by public database. Within this region, Hellenbroich Y. and his colleague found 34 different genes, and screened for mutation [4]. However, they did not find any mutation at least in the coding region of these genes.

Neuropathology has been described in one case [5]. Although only the brainstem and cerebellum was available for examination, they investigated in detail by making serial thick sections. They found that the degeneration was widespread and severe than what could be expected from ataxia and neuropathy phenotype of this disease. In the brainstem, marked neuronal loss was seen in the substantia nigra, red nucleus, ventral tegmental area, central raphe, pontine nuclei, all auditory brainstem nuclei, trochlear and abducens, principal trigeminal, spinal trigeminal, facial, superior vestibular, medial vestibular, interstitial vestibular, lateral vestibular, dorsal motor vagal, hypoglossal, and prepositus hypoglossal nuclei. Nucleus raphe interpositus, lateral reticular nuclei, reticulotegmental nucleus of the pons, the nucleus of Roller, all dorsal column nuclei, and the principal and medial subnuclei of the inferior olive were also severely affected. In the cerebellum, severe neuronal loss was seen in the Purkinje cell layer and in the fastigial nucleus. Unfortunately, spinal cord including sensory and motor nerve roots and dorsal root ganglia, and the cerebrum was not examined in this case. In addition to this, authors consider it important to wait for examinations on several other SCA4 brains to conclude the pattern of degeneration in SCA4, since clinical signs of such widespread brainstem degenerations were not reported in other patients [2]. Nevertheless, finding of widespread degeneration in this initial SCA4 autopsy case suggests that SCA4 and the chromosome 16q22.1-linked ADCA are different disease.

3. The chromosome 16q22.1-linked ADCA

The chromosome 16q22.1-linked ADCA was identified independently in Japanese. Authors (KI and HM) had collected Japanese ADCA families clinically characterized by purely cerebellar syndrome [6] (Table 1). Consistent with the clinical presentation, the magnetic resonance imaging disclosed cerebellar atrophy without obvious involvement of the brainstem (Figure 1). According to Harding's classification of ADCA, such pure cerebellar phenotype is classified as ADCA type III [7]. Screening all autosomes for 15 families with ADCA with pure cerebellar syndrome lead us to identify the first locus for the eight families to a chromosome 19p13.1-p13.2 [8]. These eight families were later diagnosed as SCA6, since they harbored trinucleotide CAG repeat expansion in the α1A voltage-dependent calcium

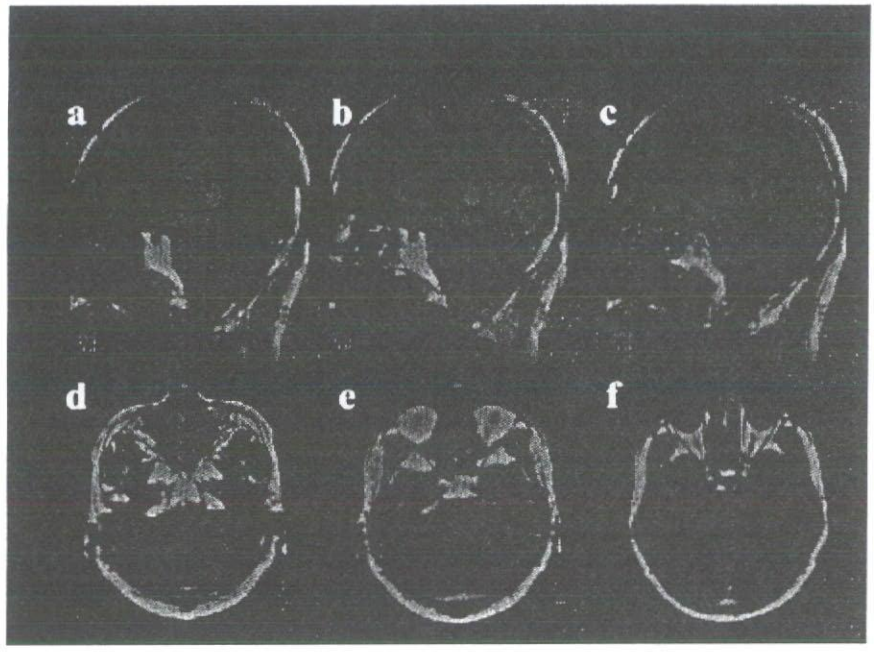

Figure 1. Magnetic resonance imaging of a patient with chromosome 16q22.1-linked ADCA. T1-weighted sagittal (a.-c.) & axial (d.-f.) brain MR images of a 58-year-old male patient 3 years after onset of ataxia. The cerebellar vermis, particularly at its upper aspect, is predominantly affected, while the brainstem is fairly well preserved.

channel gene [8-9]. We next embarked a whole genome linkage analysis for the remaining six families, and finally found that these families were linked to the *SCA4* locus in chromosome 16q13-21 [10]. This result was unexpected, since none of our families had either peripheral neuropathy or pyramidal tract signs, both of which were the clinical hallmark of SCA4. Since the clinical pictures were too distinct to consider these two diseases are allelic, we decided to coin the term "16q-linked ADCA type III" instead of a variant of SCA4.

To identify a causative gene of 16q22.1-linked ADCA, we next performed fine mapping [11], and we found a region where every patient from different families shared a same haplotype. This indicates a strong "*founder effect*" in 16q22.1-linked ADCA. Since this region with the same haplotype was demarcated by a centromeric marker, D16S3043 and a telomeric marker, D16S3095, we next constructed a physical map by independently constructing a bacterial artificial chromosome (BAC) contig [12]. By this effort, we identified several new polymorphic markers. We then applied these markers to see haplotype/allele sharing with all families, and were able to further narrow down the region with a common haplotype to a 3.8-Mb region limited by GGAA05 and D16S3095 [12].

As we collect families with ADCA type III, we encountered a large 5 generation family with 13 affected members [13]. The founder haplotype segregated with the disease in this family. Clinically, all affected individuals had

progressive cerebellar ataxia with average age of onset at 52 years. In addition, progressive hearing impairment with average age of onset at 59 years was noted in all affected individuals. During our follow-up, one of these individuals died of a natural reason at her age of 96. Detail of this patient has been described elsewhere [13-14]. To summarize, this patient noted difficulties in walking from age 70, and she gradually became ataxic. She was admitted to a nursing home at her age of 90, due to severe gait disturbance. At the age of 96, she died of natural cause. We were allowed to examine neuropathology of this patient.

Macroscopically, only the upper aspect of the vermis showed evidence of degeneration (Figure 2). Otherwise, the brain and spinal cord appeared unremarkable. Note that the degeneration appeared restricted to the upper aspect of the cerebellum, despite that the patient had the degenerative disease for 26 years. On microscopic examination, the most prominent feature was the Purkinje cell degeneration with relative preservation of molecular and granular layers. Importantly, Purkinje cells were not completely lost, but many remained with atrophic cell bodies accompanied by an amorphous structure surrounding the cell body (Figure 3). Since this amorphous material reminded us of the halo of the Lewy body, we coined the term "halo-like" amorphous structure as the peculiar Purkinje cell degeneration in 16q22.1-linked ADCA. In fact, this change was confirmed in all 16q22.1-linked ADCA patients subsequently examined neuropathologically. Since this unique feature had not been previously described, we considered that this is a neuropathological hallmark of 16q22.1-linked ADCA reflecting slow and restricted degeneration of the Purkinje cell.

Figure 2. Macroscopic view of the cerebellum of a patient with chromosome 16q22.1-linked ADCA. Consistent with MRI finding (Figure 1), degeneration is evident only at the superior vermis. Note that this individual had the disease for more than 20 years. (abopted from Ref. #15.)

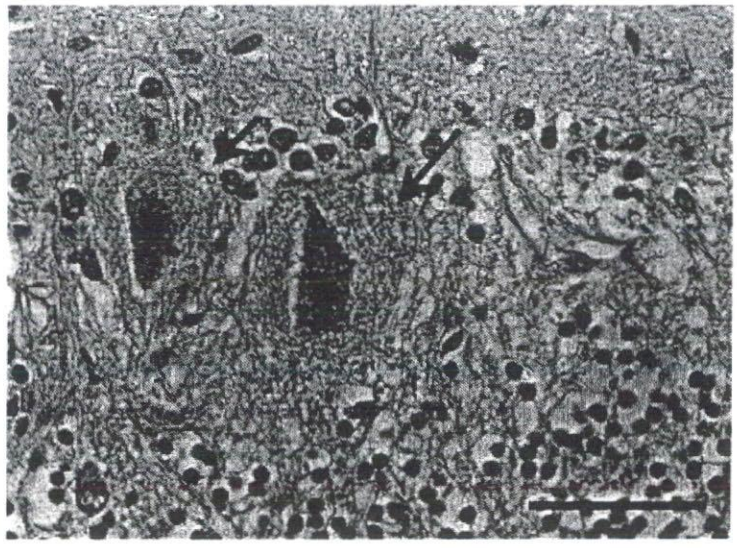

Figure 3. A peculiar Purkinje cell change in chromosome 16q22.1-linked ADCA. Note atrophic Purkinje cell bodies surrounded by so called, "halo-like" amorphous structures (arrows). (A horizontal bar measures 50 micro-meters.)

4. Identification of *puratrophin-1* genetic change in 16q22.1-linked ADCA patients

To identify the causative gene of 16q22.1-linked ADCA, we were allowed to collect 52 families from all major districts of Japan, except for Shikoku. When we further analyzed haplotypes between GGAA05 and D16S3095 [12], we prioritized the most critical interval of 16q22.1-linked ADCA to a 600 kb region between GATA01 and 17msm, because all families were found to harbor a common haplotype delimited by these two markers [15]. Twenty-two different genes were annotated in this region.

We screened all the genes annotated in this region by PCR and direct sequencing method. We also performed southern blot analysis to check for a chromosome rearrangement. From these efforts, we finally found only one genetic change which was specific for patients with 16q22.1-linked ADCA. The change was a single-nucleotide, C-to-T change seen at 16 nucleotides upstream from the putative translation initiation codon (-16C>T) of the gene, *PLEKHG4*, which we re-named as, "*puratrophin-1*"(*Purkinje cell atrophy associated protein-1*)[15](Figure 4).

Clinical features of 16q22.1-linked ADCA on 52 families were compared with those of SCA4 families (Table 1). As a definition, our families were purely cerebellar syndrome, except that approximately 40% of patients also showed hearing impairment. Notably, this symptom may be very subtle that it could only be noticed by testing with audiogram. Other groups also examined clinical features of 16q22.1-linked ADCA [16-17]. They also found that patients show

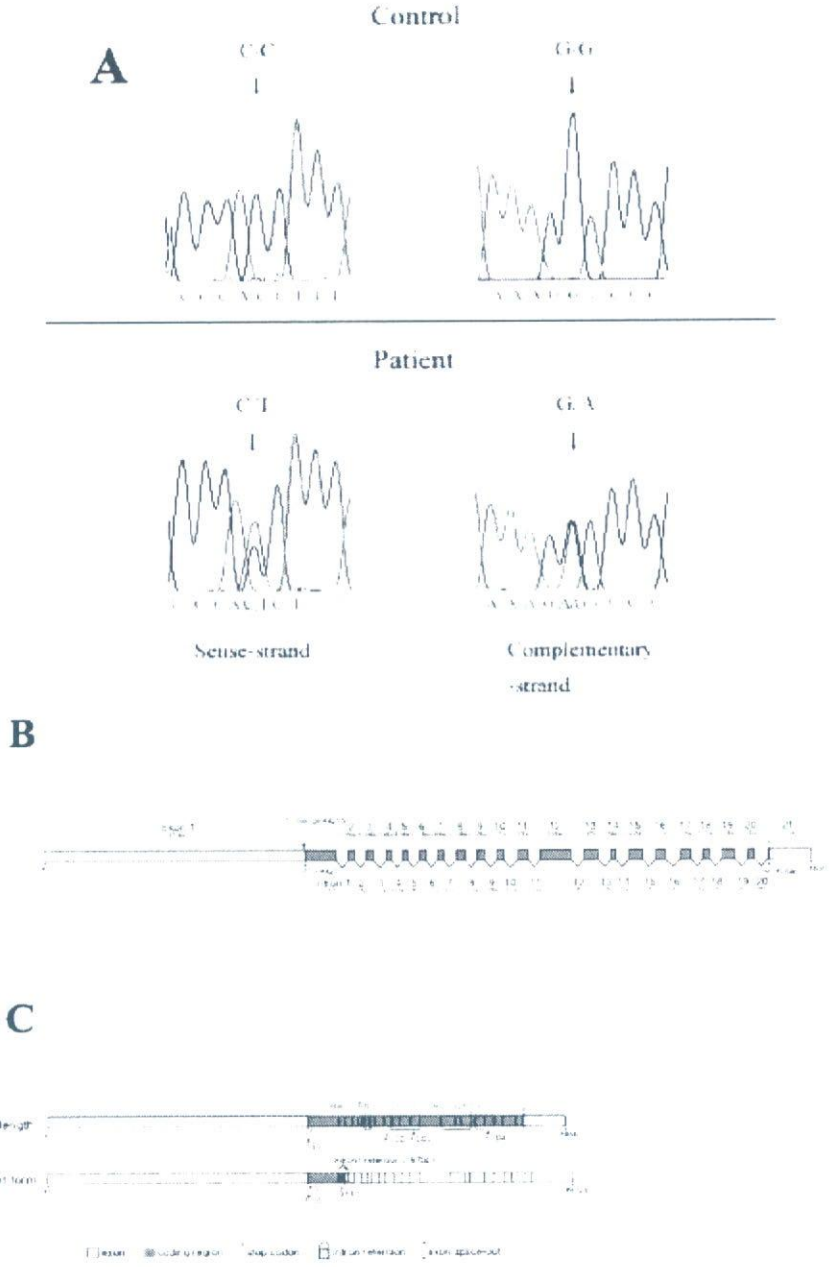

Figure 4. A -16C>T single-nucleotide change in the *puratrophin-1* gene highly associated with chromosome 16q22.1-linked ADCA. A. A single-nucleotide cytosine (C) to thymine (T) change is seen in the sense strand of patient's DNA. B. Genomic structure of the *puratrophin-1* gene. C. Full-length and short-form *puratrophin-1* mRNA. The full-length puratrphin-1 mRNA has four major domains, CRAL-TRIO, spectrin repeat, guanine nucleotide exchange factor for Rho/Rac/Cdc42-like GTPases (Rho GEF), and pleckstrin homology (PH) domains. (A-C. all adopted from Ref. #13)

"purely" cerebellar syndrome. These studies also showed that the disease frequency of 16q22.1-linked ADCA is about 10% of all ADCA in Japan. This means that 16q22.1-linked ADCA is frequent subform of ADCA, next to Machado-Joseph disease and SCA6.